

Review

# Progress and Trend on the Regulation Methods for Nanozyme Activity and Its Application

Li Hou, Gaoyan Jiang, Ying Sun, Xuanhan Zhang, Juanjuan Huang, Shendong Liu, Tianran Lin \* , Fanggui Ye  and Shulin Zhao \*

State Key Laboratory for the Chemistry and Molecular Engineering of Medicinal Resources, College of Chemistry and Pharmaceutical Science, Guangxi Normal University, Guilin 541004, China; houli@gxnu.edu.cn (L.H.); gyj18778313889@163.com (G.J.); Sunying33252@163.com (Y.S.); zxh281784100@hotmail.com (X.Z.); hjj97218@163.com (J.H.); shendong2013@163.com (S.L.); fangguiye@163.com (F.Y.)

\* Correspondence: tianranlin@163.com (T.L.); zhaoshulin001@163.com (S.Z.)

Received: 26 November 2019; Accepted: 9 December 2019; Published: 12 December 2019



**Abstract:** Natural enzymes, such as biocatalysts, are widely used in biosensors, medicine and health, the environmental field, and other fields. However, it is easy for natural enzymes to lose catalytic activity due to their intrinsic shortcomings including a high purification cost, insufficient stability, and difficulties of recycling, which limit their practical applications. The unexpected discovery of the Fe<sub>3</sub>O<sub>4</sub> nanozyme in 2007 has given rise to tremendous efforts for developing natural enzyme substitutes. Nanozymes, which are nanomaterials with enzyme-mimetic catalytic activity, can serve as ideal candidates for artificial mimic enzymes. Nanozymes possess superiorities due to their low cost, high stability, and easy preparation. Although great progress has been made in the development of nanozymes, the catalytic efficiency of existing nanozymes is relatively low compared with natural enzymes. It is still a challenging task to develop nanozymes with a precise regulation of catalytic activity. This review summarizes the classification and various strategies for modulating the activity as well as research progress in the different application fields of nanozymes. Typical examples of the recent research process of nanozymes will be presented and critically discussed.

**Keywords:** nanozyme; activity regulation; artificial mimic enzyme

## 1. Introduction

All life phenomena in nature are related to enzymes. Almost all chemical reactions occurring in living cells are catalyzed and controlled by enzymes. Enzymes are a type of biomacromolecule with biocatalytic function, which can tune the metabolism of organic organisms, transmitting genetic information, sustaining life activities, and catalyzing chemical reactions. Owing to their excellent catalytic efficiency and strong substrate specificity, enzymes are widely used in biosensors, medicine and health, environmental protection, and other fields. However, due to the shortcomings of most natural enzymes, such as their poor stability, time-consuming preparation, and high preparation costs, there is great significance for practical application to design and synthesize stable and low-cost artificial mimetic enzymes to replace natural enzymes by full chemical synthesis or semi-synthetic methods [1–5].

Artificial mimetic enzymes are also known as one of the important branches of bionics; they refer to the use of artificial materials to simulate the structure and function of natural enzymes, and they were first proposed by Ronald Breslow [1,2]. In the past decades, great progress has been made in the field of mimetic enzymes [3,4]. A series of mimetic enzymes have been synthesized, such as cyclodextrins, metal complexes, porphyrins, and biological molecules, and used as substitutes for natural enzymes in various fields [5,6]. Compared with natural enzymes, these traditional mimetic

enzymes have the advantages of simple structure, low molecular weight, and high stability (especially at high temperature). However, their low catalytic activity and poor selectivity are common problems of traditional mimetic enzymes.

Scrimin and Pasquato and their coworkers found that gold nanoparticles modified by azacrown had a nuclease-like function and could catalyze the phosphodiester bonds of nucleic acids [7]. Then, they first proposed the concept of the “nanozyme” to describe this monolayer of thiol-protected gold nanoclusters with significant ribonuclease activity, which was later extended to describe nanomaterials with enzymatic activity. In 2007, the Yan group reported for the first time that magnetic iron tetroxide nanoparticles exhibited peroxidase-like properties [8]. This discovery has attracted widespread attention to the nanozyme, which has rapidly become a research hotspot. Hui Wei and Erkang Wang further defined the concept of nanozyme as “nanomaterials with enzymatic properties”. As a new generation of artificial mimetic enzymes, nanozymes are more stable and economical than natural enzymes and traditional artificial enzymes. So far, a variety of nanozymes have been reported and widely used in the fields of biosensors, environmental remediation, and disease treatment [5,6].

## 2. Types and Classification of Nanozymes

Until now, many nanomaterials have been found to possess enzyme-mimic activity. Considering the dual characteristics of nanozymes, i.e., nanomaterials and catalysts, the nanozymes can be classified by the nanomaterial's dimensions and catalytic types. Firstly, it can be classified by the nanomaterial's dimensions. If three dimensions of a nanomaterial are in the nanoscale (usually less than 100 nm), it can be named as a zero-dimensional nanozyme [9–19]. If two dimensions of a nanomaterial are in the nanoscale, it can be named as a one-dimensional nanozyme [20–26]. In the same way, there are also two-dimensional nanozymes (one dimension in the nanoscale) [27–34] and three-dimensional nanozymes (zero dimension in the nanoscale) [35–43]. Secondly, according to the types of enzymatic reactions, we can name nanozymes according to their mimetic natural enzymes, including peroxidase nanozyme, catalase nanozyme, oxidase nanozyme, nitrate reductase nanozyme, nuclease nanozyme, and so on.

## 3. Regulation Strategy of Nanozyme Activity

Similar to natural enzymes, the activity of nanozymes can be regulated in different ways, including according to their material size, composition, morphology, surface modification, pH and temperature, and activators or inhibitors. This section summarizes and discusses the above-mentioned important factors for influencing the catalytic performance of nanozymes.

### 3.1. Size

Size is a key factor in determining many properties of nanomaterials. Generally, the catalytic activity of nanozymes can be regulated by controlling the size. In most cases, smaller nanoparticles have higher activity, which is probably due to their having a larger specific surface area. In other words, the catalytic activity of nanozymes increases with the increase of the specific surface area. Some studies have shown that the catalytic activity of one nanozyme is related to its size [44–46]. The Peng group studied the peroxidase catalytic activity of  $\text{Fe}_3\text{O}_4$  NPs with average diameters of 11, 20, and 150 nm [47]. It was found that the peroxidase catalytic activity of  $\text{Fe}_3\text{O}_4$  NPs increased with the decrease of the diameters of nanoparticles. Asati et al. obtained similar results when studying the oxidase activity of organic polymer-modified cerium oxide nanoparticles with different sizes of 5, 12, 14, and 100 nm [48]. Therefore, the catalytic activity of nanozymes can be achieved by tuning the size of the nanozymes.

### 3.2. Morphology

The shape and morphology of nanozymes plays a key role in regulating their catalytic activity [49–52]. Tian et al. have investigated the effect of different morphologies (nanosheets, nanofibers, and nanorods) of  $\text{VO}_2$  nanoparticles on the colorimetric assay for  $\text{H}_2\text{O}_2$  and glucose [53].

It is found that VO<sub>2</sub> nanofibers exhibit the highest peroxidase-like activity, since the specific surface area of VO<sub>2</sub> nanofibers is much larger than that of VO<sub>2</sub> nanosheets and nanorods. To illuminate the morphology effects on the catalytic ability of Mn<sub>3</sub>O<sub>4</sub> nanoparticles, Singh et al. studied the size, pore size, surface area, and volume of the various morphologic Mn<sub>3</sub>O<sub>4</sub>, including nanoflowers, cubes, polyhedron, hexagonal plates, and flakes (Figure 1) [54]. The results showed that Mn<sub>3</sub>O<sub>4</sub> nanoflowers exhibited higher catalytic activity than that of other morphologic Mn<sub>3</sub>O<sub>4</sub> nanomaterials due to their higher surface area and larger size as well as the bigger pore size of the Mn<sub>3</sub>O<sub>4</sub> nanoflowers. Additionally, the effects of the morphology of Co<sub>3</sub>O<sub>4</sub> [55], Fe<sub>3</sub>O<sub>4</sub> [56], MnO<sub>2</sub> [57], LaNiO<sub>3</sub> [42], and CoFe<sub>2</sub>O<sub>4</sub> [58] on their catalytic activity have also been reported.

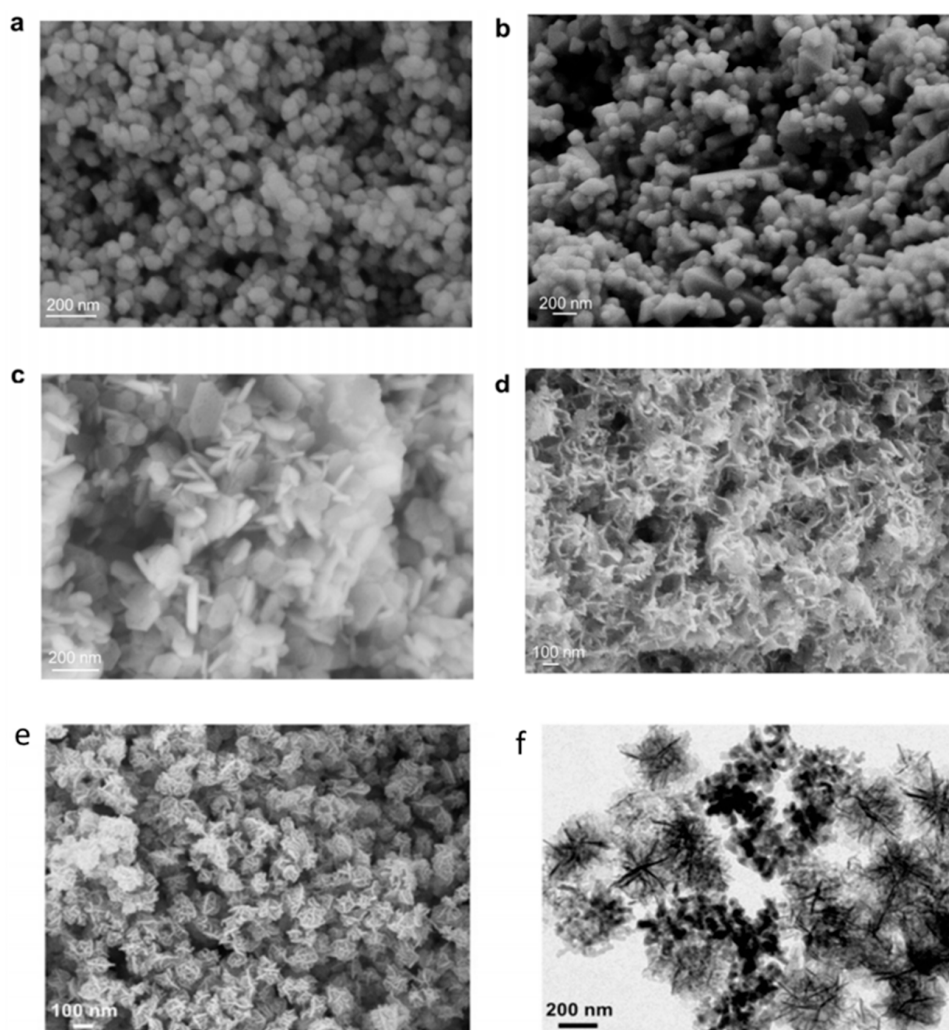


**Figure 1.** (a–e) SEM images of different morphologic Mn<sub>3</sub>O<sub>4</sub> including the cubes, polyhedrons, hexagonal plates, flakes, and flowers, respectively. (f) TEM image of Mn<sub>3</sub>O<sub>4</sub> nanoflowers. Reproduced from Reference [54] with permission from Wiley.

### 3.3. Composition

The components of nanozymes can effectively affect the catalytic activity. Doping methods and a constructing complex is often used to regulate the activity of nanozymes [59–64]. He et al. found that the simulated superoxide dismutase (SOD) activity of the CeO<sub>2</sub> nanozyme decreased with the doping amount of titanium, which suggested that the SOD activity was easily affected by the spheroidal nanostructure, and Ti-doping promoted a conversion from the cubic crystal phase of CeO<sub>2</sub> to a spheroidal nanostructure [65]. On the contrary, the oxidase-like activity of CeO<sub>2</sub> was somewhat enhanced by Ti doping. Two kinds of catalytic activities of Ti-doping CeO<sub>2</sub> were different,

because SOD activity appeared to be sensitive to the spheroidal nanostructure, while the oxidase-like activity did not. What's more, the combination of two or more similar functional nanomaterials can effectively improve the catalytic efficiency compared to the individual nanomaterial. In contrast with the individual AuNPs and Fe<sub>3</sub>O<sub>4</sub> NPs, their composites exhibit higher peroxidase activity, which can be attributed to three factors: the synergistic effect [60], the polarization effect of AuNPs to Fe<sub>3</sub>O<sub>4</sub> [66], and the special electronic structure interface between Fe<sub>3</sub>O<sub>4</sub> and AuNPs [67]. However, the less active core could be etched for the aim of growing the higher active sites and further improving the catalytic activity of nanomaterial. Wu et al. synthesized Pt hollow nanodendrites with the more active sites and high-index facets that were derived from Pd–Pt core–frame nanodendrites, and then etched the Pd core, exhibiting the enhancement of peroxidase-like activity (Figure 2) [68].

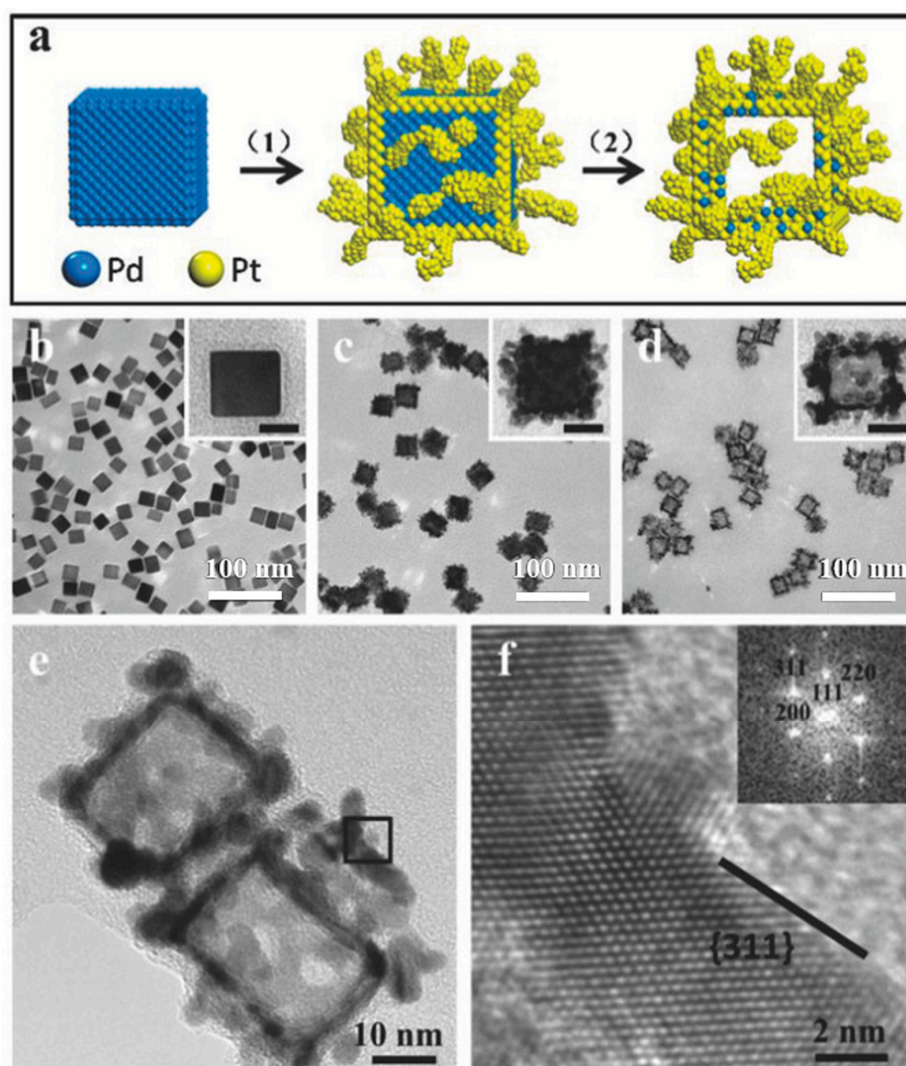


**Figure 2.** (a) The formation of Pt hollow nanodendrites including the (1) deposition process of Pt atoms for the generation of Pd@Pt core–frame nanodendrites and the (2) etching process of Pd cores using FeBr<sub>3</sub>. (b–d) TEM images of Pd nanocubes, Pd@Pt core–frame nanodendrites, and Pt hollow nanodendrites, respectively. (e) TEM image of Pt hollow nanodendrites with hollow interiors and abundant branches. (f) HRTEM image taken from the corner region of a Pt hollow nanodendrite. The corresponding FT pattern is shown in the inset. Reproduced from Reference [68] with permission from Wiley.

### 3.4. Surface Modification

The surface modification can be achieved by covalently immobilizing functional groups and electrostatic adsorption. After surface modification, nanozymes possessed different catalytic abilities and delivered the required performances for further biological coupling [8]. Generally, if the number of active sites that can bind with the substrate is reduced by the surface modification method, it will decrease the catalytic activity of a nanozyme. Gao et al. studied the  $\text{Fe}_3\text{O}_4$  NPs coated with 3-aminopropyltriethoxysilane, polyethylene glycol, dextran, and silica [8]. It was found that the peroxidase activity of these coated  $\text{Fe}_3\text{O}_4$  NPs was generally lower than that of unmodified  $\text{Fe}_3\text{O}_4$  NPs. However, some coatings can also improve the catalytic activity of nanozymes. Zhang et al. found that the peroxidase-like activity of Prussian blue-coated  $\gamma\text{-Fe}_2\text{O}_3$  NPs increased significantly [69]. They attributed the reason to two points: the surface charge of the coated  $\gamma\text{-Fe}_2\text{O}_3$  NPs was changed from positive charge to negative charge and the substrate-binding was enhanced by electrostatic interaction; in addition, more ferrous active centers were introduced by Prussian blue. However, it is noteworthy that Prussian blue itself has peroxidase activity. Qu's group studied the effect of surface functional groups on peroxidase activity in graphene quantum dots (GQD) (Figure 3) [14]. Carbonyl, hydroxyl, and carboxyl groups on the surface of GQD were selectively modified by benzoic anhydride (BA), phenylhydrazine (PH), and 2-bromo-1-phenylethyl ketone (BrPE), respectively. Compared with unmodified GQD, the peroxidase activity of GQDs-BA and GQDs-BrPE was increased, while the peroxidase activity of GQDs-PH was inhibited. Using terephthalic acid, they found that the carbonyl group on GQD was the active site, the carboxyl group was the substrate-binding site, and the hydroxyl group inhibited the activity of the enzyme. This discovery explains the mechanism of carbon materials as peroxidase mimetic enzymes, providing a solid theoretical basis for the design and synthesis of carbon materials in the future. Therefore, surface modification acts as one of the effective methods to regulate the catalytic efficiency of nanozymes.

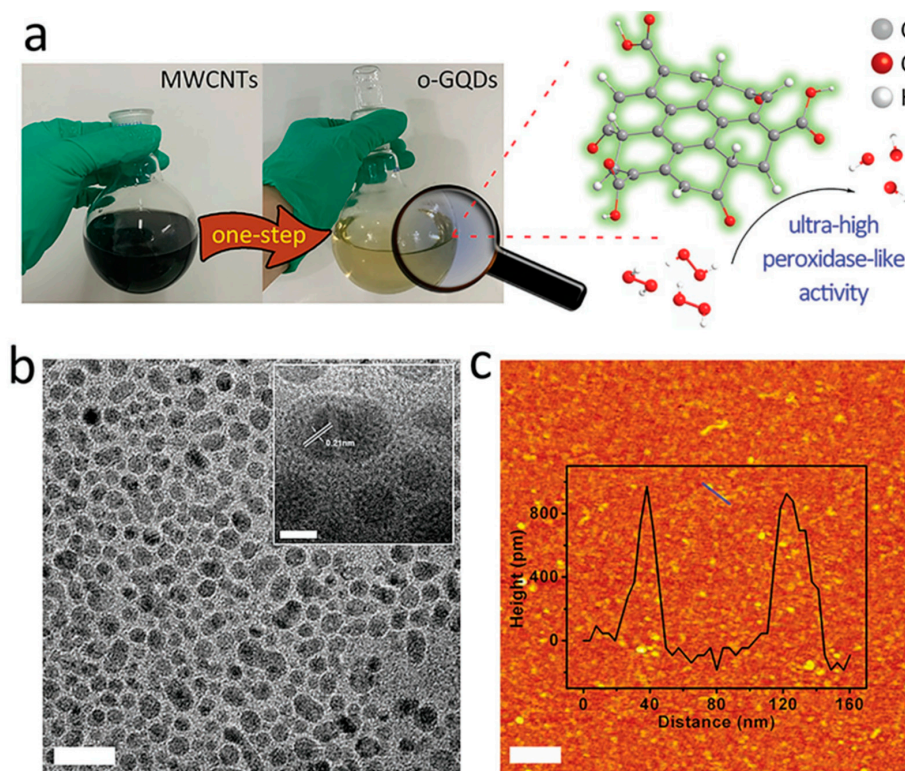


**Figure 3.** (a) Schematic representation of the preparation of graphene quantum dots (GQDs). (b) TEM image of GQDs. The scale bar is 20 nm. (c) Atomic force microscope image of GQDs. Reproduced from Reference [14] with permission from Wiley.

### 3.5. pH and Temperature

The pH factor plays an important role in the reactions catalyzed by nanozymes. It was found that some nanozymes exhibited different enzyme activities at different pH values [70–73]; for example, if the pH of  $\alpha$ -ZrO<sub>2</sub> is lower than 5.3, it shows the catalytic activity of peroxidase, and when the pH is higher than 5.3, it shows the catalytic activity of catalase [71]. Additionally, the temperature factor can also regulate the catalytic efficiency of nanozymes. Qu's group designed bovine serum albumin (BSA) as the model protein to construct the BSA–Cu<sub>3</sub>(PO<sub>4</sub>)<sub>2</sub>·3H<sub>2</sub>O hybrid nanoflower. In the temperature range from 15 to 65 °C, the nanoflowers showed high-temperature catalytical activity compared with the natural horseradish peroxidase (HRP) under the same condition [74]. More interestingly, the catalytic activity of the nanoflower was improved with the increment of temperature. Additionally, Qu's group performed an interesting study on pH and temperature modulation [75]. A dual photoresponsive system for the photoregulation of chemical reactions based on the combination of ultraviolet (UV) and near-infrared (NIR) light-sensitive materials were developed. The achievement of regulatory effect was via the modulation of reaction temperature and pH. The hybrids of the photobase reagent malachite green carbinol base (MGCB) and graphene oxide were used for the photoregulation of pH and temperature. Under the stimulation of ultraviolet and near-infrared light, high temperature from graphene oxide and OH<sup>−</sup> from MGCB were produced, respectively. Accordingly, the change of pH and temperature were tuned under irradiation, resulting in the modulation of the catalytic activities of nanozyme. By using nanozyme and enzyme-mediated chemical reactions as models, they verified the feasibility and high performance of this method (Figure 4) [75].

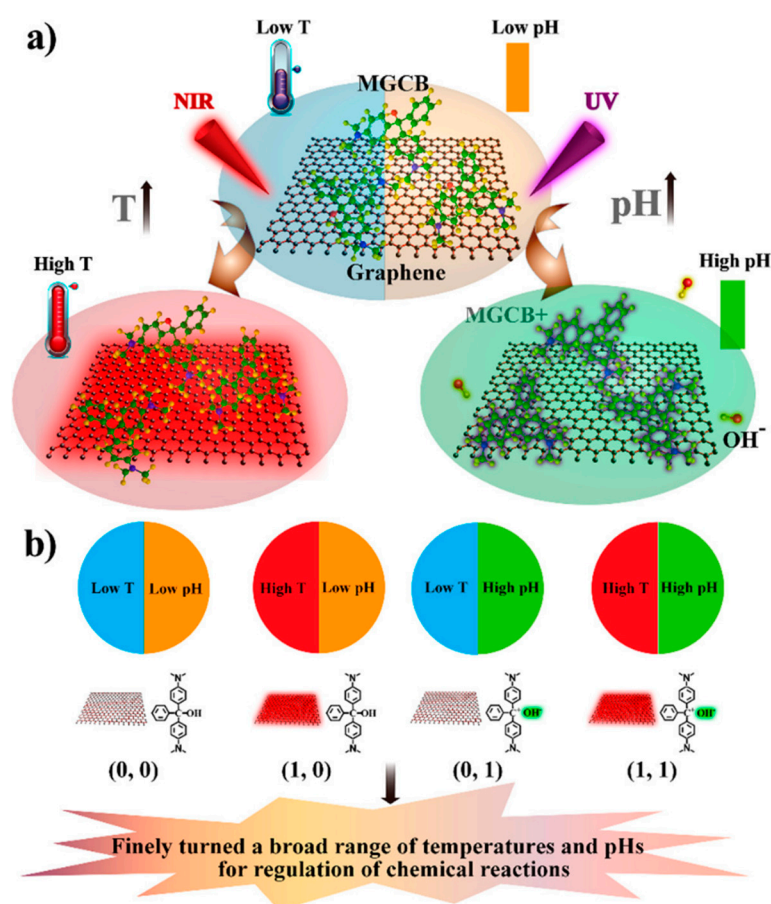


**Figure 4.** (a) Photothermal effect of graphene and light-induced pH changing the effect of malachite green carbinol base (MGCB). (b) Finely tuned a broad range of temperatures and pHs for the regulation of chemical reactions. Reproduced from Reference [75] with permission from The American Chemical Society.

### 3.6. Activators and Inhibitors

Apart from the above factors, activators and inhibitors also affected the catalytic performance of nanozymes [76–79]. For natural enzymes, activators can increase the activity of enzymes, while inhibitors can decrease the activity of enzymes. Inspired by this, researchers are also trying to find activators and inhibitors to regulate the catalytic activity of nanozymes. In some cases, certain ions and other molecules could react with the nanozymes to affect the catalytic activity of nanozymes. Singh's studies have shown that phosphate ions can keep Ce in the +3 valence state, increasing the catalase-like activity of nano-cerium dioxide [59]. Liu et al. carried out a series of screening experiments to select the optimum condition to inhibit the activity of Au@Pt nanorod oxidase [80]. It found that  $\text{Fe}^{2+}$  was an irreversible inhibitor, while  $\text{Cu}^{2+}$  and  $\text{NaN}_3$  were reversible inhibitors. Additionally, it was found that  $\text{Hg}^{2+}$  was an effective inhibitor, and a method for detecting  $\text{Hg}^{2+}$  inhibition was established.

Herein, some regulation strategies of typical nanomaterials and their applications were summarized in Table 1.

**Table 1.** The regulation strategy of typical nanomaterials and their applications. BSA: bovine serum albumin.

Types of Nanozymes	Nanomaterial	Regulation Strategy	Application	Reference
zero dimension	$\text{CeO}_{2-x}$	size (4.5 nm, 7.8 nm, 23 nm, and 28 nm); composition (surface area concentration of $\text{Ce}^{3+}$ )	decomposition of $\text{H}_2\text{O}_2$	44
	$\text{Fe}_3\text{O}_4$ NPs	size (11 nm, 20 nm, 150 nm)	catalyze the oxidation of the substrate TMB by $\text{H}_2\text{O}_2$	47
	dextran-coated nanoceria	size (5 nm, 12 nm, 14 nm, 100 nm)	enzyme-linked immunosorbent assay	48
	Au- $\text{Fe}_3\text{O}_4$ NPs	composition (complex)	detection of $\text{H}_2\text{O}_2$	60
	Ti-doped $\text{CeO}_2$	composition (doping)	biological applications	65
	Pt hollow nanodendrites	composition (etching)	antibacteria	68
	$\text{Fe}_3\text{O}_4$	surface modification (3-aminopropyltriethoxysilane, polyethylene glycol, dextran, and $\text{SiO}_2$ )	immunoassay	8
	graphene quantum dots	surface modification (phenylhydrazine, benzoic anhydride, and 2-bromo-1-phenylethyl ketone)	glucose detection	14
	$\gamma\text{-Fe}_2\text{O}_3$ NPs	surface modification (Prussian blue)	immunoassay	69
	Ag	activator (mercury (II))	colorimetric assays for mercury (II)	76
	Pt	inhibitor (mercury (II))	colorimetric assays for mercury (II)	77
	$\text{Au}_x\text{Pt}_y$ -DNA	inhibitor (biothiol)	colorimetric assay of biothiols	78
	Pt-apoferritin	inhibitor of catalase activity ( $\text{NaN}_3$ ), inhibitor of catalase and superoxide dismutase activities (3-amino-1,2,4-triazole)	engineering targeting enzyme mimetics	79
	$\text{CeO}_2$	inhibitor (phosphate)	catalyst	59
	Prussian Blue	pH	multienzyme mimetics and reactive oxygen species scavengers	71
	$\text{CoFe}_2\text{O}_4$	pH, surface modification	chemiluminescence without the need for $\text{H}_2\text{O}_2$	73
	one dimension	$\text{VO}_2$	morphology (nanofibers, nanosheets, and nanorods)	detection of $\text{H}_2\text{O}_2$ and glucose
$\text{Mn}_3\text{O}_4$ nanoflower		morphology (nanoflowers, cubes, polyhedron, hexagonal plates, and flakes)	preventing the cells from oxidative damage	54
$\text{Co}_3\text{O}_4$ nanoplates		morphology (nanoplates, nanorods, and nanocubes)	determination of calcium ion	55
Au@Pt nanorods		inhibitor ( $\text{Fe}^{2+}$ , $\text{Cu}^{2+}$ , and $\text{NaN}_3$ )	screening of inhibitors for oxidase mimics	80
two dimension	graphene oxide	pH, temperature	programmable wound healing	75
	$\text{WS}_2$	temperature	glucose detection	31
three dimension	$\text{ZrO}_2$ gel	pH	nonredox system construction	70
	BSA- $\text{Cu}_3(\text{PO}_4)_2 \cdot 3\text{H}_2\text{O}$	temperature	decompose organic pollutants	74

## 4. Applications of Nanozymes

### 4.1. Nanozymes in Antibacteria for Topical Application

Up to now, the usage of nanozymes in combatting multi-drug resistant bacteria and biofilms has become an attractive field. Metal oxide-based and sulfide metal-based nanozymes, carbon-based enzymes, and nanocomposites show good biocompatibility and antibacterial activities, which have been applied for killing bacteria [3]. However, most related works about nanozyme antibacterial agents were applied for topical applications such as mouse skin, since they would release reactive oxygen species (ROS) in an aspecific manner. Therefore, nanozymes for antibacterial applications cannot be systemically administered until now. Although the antibacterial and antibiofilm mechanism of nanozymes are largely unknown, three aspects are mainly summarized as following [3]: (1) nanozymes trigger the generation of reactive oxygen species (ROS) such as hydroxyl radical ( $\bullet\text{OH}$ ) and superoxide anion ( $\text{O}_2^{\bullet-}$ ), which can attack bacteria and biofilms because of the high oxidation capability of ROS [81], and unselectively defunctionalize many important substances such as lipids, proteins, and nucleic acids, thus causing the lysis of the bacterial cytoplasmic membrane, protein deactivation, and DNA damage. (2) Deoxyribonuclease mimics, as a kind of hydrolytic nanozymes, can catalytically cleave the extracellular DNA for inhibiting the formation of biofilms and dispersing the integrity of the biofilm [82]. (3) Haloperoxidase mimics that can reduce autoinducers have exhibited a successful inhibition of biofilm growth and the destruction of biofilms [83]. However, most of the existing antibacterial mechanism was focused on the above first one. Karim et al. reported that CuO nanorods could serve as high-efficiency antibacterial agents under light illumination, which causes a 20 times enhancement of the  $\bullet\text{OH}$  production rate compared with the dark condition [84]. Yan's group first demonstrated a zinc-based zeolitic-imidazolate-framework (ZIF-8) derived Zn-N-C single-atom nanozyme (SAzyme) that is considered as a high therapeutic effect single-atom catalyst for wound antibacterial application (Figure 5) [85]. The high catalytic activity of the SAzyme was due to the coordinatively unsaturated Zn-N<sub>4</sub> active site, leading to the dissociation of H<sub>2</sub>O<sub>2</sub> and the generation of  $\bullet\text{OH}$ . The formation of high oxidative  $\bullet\text{OH}$  could trigger the oxidation of cellular components and then result in the bacteria apoptosis. The result showed that the inhibition rate of the SAzyme on bacteria was 99.87%. Moreover, the SAzyme significantly promoted wound healing with low toxicity to the organism.

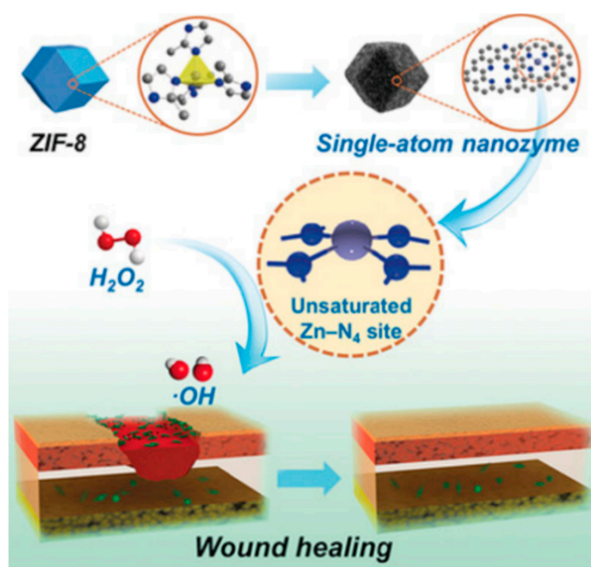


**Figure 5.** Schematic representation of zinc-based zeolitic-imidazolate-framework (ZIF-8) derived Zn-N-C single-atom nanozyme for wound antibacterial application. Reproduced from Reference [85] with permission from Wiley.

#### 4.2. Nanozymes in Hazardous Degradation

Organic pollutants, especially those with high toxicity, have shown serious effects on the eco-environment system and human health [86]. The degradation of organic pollutants for decreasing environmental pollution has been a focus of attention of the international community. Until now, a variety of methods have been proposed to decompose organic pollutants, including chemical oxidation, physical adsorption, and biological degradation. Among them, physical adsorption is not an ideal method, since it lacks the efficiency in the process and needs abundant adsorbing materials [87]. For chemical oxidation, it needs a Fenton reagent including  $\text{Fe}^{3+}$ ,  $\text{Fe}^{2+}$ , and  $\text{H}_2\text{O}_2$ . However, chemical oxidation usually produces iron ions and sludge, which were easily discharged into the environment, resulting in secondary pollution [88,89]. Biological degradation has the properties of being highly efficient and environmentally friendly. Nevertheless, the natural enzyme which is applied for biological degradation is expensive and unstable. Thus, it is urgent to explore new materials and methods to decompose organic pollutants. The nanozyme is an ideal degradation agent. So far, the reported organic molecules of nanozyme degradation include phenol, bisphenol A, methyl blue, sulfamethoxine, 4-chlorophenol, norfloxacin, xylene orange, sulfathiazole, rhodamine B, methylene blue, and congo red. Wang et al. prepared a novel CH-Cu nanozyme based on the coordination of  $\text{Cu}^+/\text{Cu}^{2+}$  with a Cys-His dipeptide for the degradation of chlorophenols and bisphenols (Figure 6) [90]. The CH-Cu nanozymes can mimic the laccase activity and exhibit an excellent catalytic activity, recyclability, and substrate universality comparable with laccase. Employing key peptides as metal ligands for the metal ions complexing reaction is a novel concept and method for the design and synthesis of new nanozymes, which could mimic the structure of the active site of a natural enzyme. Despite this process, an enormous challenge is the immobilization of nanozymes, since attaching ligands to nanozymes may block active sites and affect their catalytic activity [91]. To solve this problem, the idea of growing a layer of nanozymes on magnetic nanoparticles is proposed, which could be a benefit for separation and recycling as well as the maintaining of catalytic activity. Zhang et al. reported a novel magnetic laccase-like nanozyme ( $\text{Fe}_3\text{O}_4@/\text{Cu}/\text{guanosine } 5'-\text{monophosphate (GMP)}$ ), which could oxidize harmful *o*-phenylenediamine and remove phenolic compounds [92]. Based on the complexed  $\text{Cu}^{2+}$  and GMP, which possessed the laccase-like activity and were modified on the outside of  $\text{Fe}_3\text{O}_4$  nanoparticles, the catalytic performance of  $\text{Fe}_3\text{O}_4@/\text{Cu}/\text{GMP}$  was achieved. The application of magnetic nanoparticle as a magnetic core is conducive to further separation and recycling. Besides, the photocatalytic degradation of organic pollutants generally takes place in a stepwise fashion [93]. Photocatalytic degradation can occur under ultraviolet (UV) or visible light irradiation, causing the degradation of organic pollutants. Fan et al. reported an efficient titanate nanomaterials (NTs) photocatalyst modified with  $\text{H}_2\text{O}_2$  (HTNM), exhibiting an enhanced photoresponse to visible light with high photocatalytic activity for the degradation of naproxen [94]. These above reports show that nanozymes can potentially be a substitution for natural enzymes in hazardous degradation and environmental remediation.

#### 4.3. Nanozymes in Sensing

Nanozymes have been extensively explored for the sensing of various important targets in the fields of food safety analysis, environmental monitoring, disease diagnosis, and pharmaceutical analysis, ranging from food and environmental pollutants, bioactive small molecules, metal ions, nucleic acids, biomarkers, and cancer cells. Nevertheless, the simultaneous analysis of multiple targets by using one single nanozyme is still a challenge. To solve this problem, the Qu group established a multiplex readout method for the pattern recognition of different proteins by using graphitic carbon nitride ( $\text{g-C}_3\text{N}_4$ ) nanosheets as a single sensing receptor with peroxidase-like activity (Figure 7) [95]. It is surprising that the catalytic activity of  $\text{g-C}_3\text{N}_4$  nanosheets can be regulated into different degrees because of the different interactions between  $\text{g-C}_3\text{N}_4$  and proteins. The advantage of this platform is no need for numerous sensing receptors and sophisticated instruments, resulting in lower cost and time consumption, providing a new pathway for the construction of convenient, feasible, and flexibly nanozyme-based sensing arrays. The  $\text{g-C}_3\text{N}_4$ -based nanozyme is not only used for the construction

of colorimetric sensors, but it can also be used for fluorescent sensors. However, the fluorescence performances at a single emission wavelength are easily affected by environmental factors, such as exciting and emitting light efficiency, and fluorescence probe concentration [96]. The ratio of double emission wavelengths is obtained as a response signal that improves the accuracy of the results by the self-calibration of two different emission wavelengths. The Wei group designed the ratiometric sensing systems by using three kinds of fluorescent  $C_3N_4$ -based nanozymes such as  $C_3N_4$ -Ru,  $C_3N_4$ -Cu, and  $C_3N_4$ -hemins, which possessed excellent peroxidase mimic catalytic activities [97]. The fluorescent intensity at 438 and 564 nm as the signal output was used to construct ratiometric sensor assays for the determination and discrimination of five phosphates, providing more reliable and robust sensing performance.

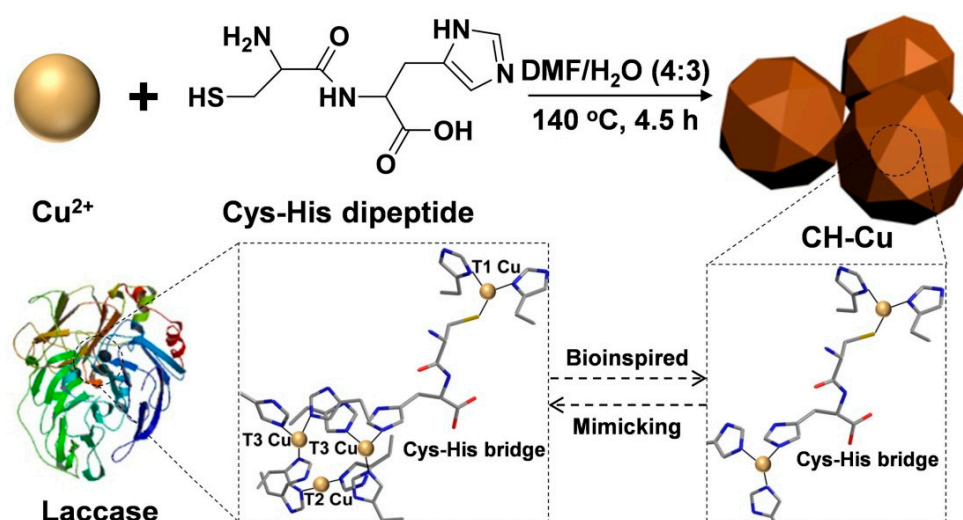


**Figure 6.** Schematic representation of a new CH-Cu nanozyme via the coordination of  $Cu^+$ / $Cu^{2+}$  with a Cys-His dipeptide for the degradation of chlorophenols and bisphenols. Reproduced from Reference [90] with permission from Elsevier.

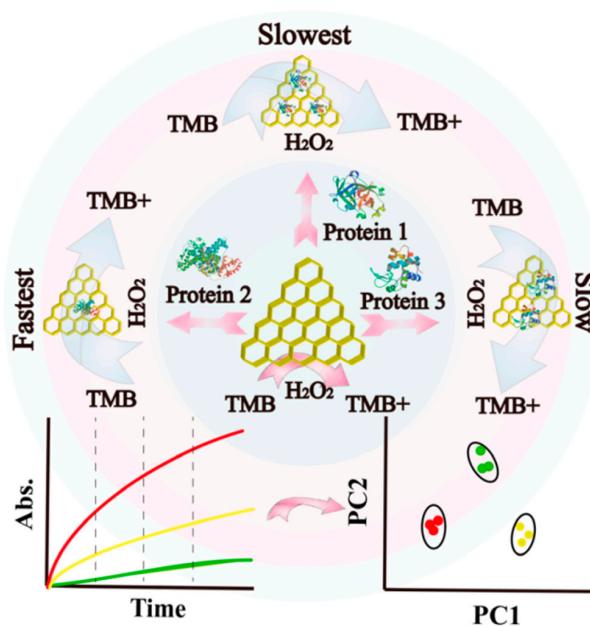


**Figure 7.** Schematic representation of one kind of multiple readout system based on g- $C_3N_4$  nanosheets for the recognition of different proteins. Reproduced from Reference [95] with permission from The American Chemical Society.

#### 4.4. Nanozymes in Cancer Therapy

In cancer diagnosis and therapy, nanozymes have received great attention. Nanozymes can be remotely controlled by different stimuli such as magnetic field, light, ultrasound, and heat [98]. These above stimuli factors can be applied for improving the diagnostic and therapeutic efficacies of different diseases in biomedical applications. For example, Li et al. developed a PtFe@Fe<sub>3</sub>O<sub>4</sub> nanozyme with two kinds of enzyme-like catalytical activities for tumor therapy [99]. In the tumor microenvironment, the PtFe@Fe<sub>3</sub>O<sub>4</sub> nanozymes exhibited a photothermal effect with photo-enhanced catalase-like and peroxidase-like activities. The current systems are mainly based on oxygen status and/or external stimuli to produce ROS, which can cause the apoptosis of tumor cells and act as a promising treatment strategy for malignant neoplasms. However, for hypoxic tumors, the therapeutic efficacy is limited, because the generation of ROS highly relied on oxygen status and external stimuli. A self-assembly of MnO<sub>2</sub>@PtCo nanoflowers-based nanozymes that catalyzed a cascade of intracellular reactions to generate ROS in both normoxic and hypoxic conditions which were dispensed with external stimuli were rationally designed and synthesized by the Qu group [100] (Figure 8). PtCo and MnO<sub>2</sub> served as an oxidase mimic and catalase mimic, respectively. The MnO<sub>2</sub>@PtCo nanoflowers can relieve hypoxic conditions as well as induce the apoptosis of tumor cells based on the ROS-mediated mechanism, thus causing a remarkable and specific inhibition of neoplasm growth. In contrast with traditional ROS-mediated systems, this platform possesses many advantages; for example, no external stimuli were needed. By combining the oxidative activity of PtCo with the supplement ability of O<sub>2</sub> from MnO<sub>2</sub>, remarkable therapeutic efficacies for hypoxic tumors were achieved. The MnO<sub>2</sub>@PtCo nanoflowers could preferentially cause the apoptosis of tumors, since the oxidative ability of nanoflowers depends on the acidic pH.

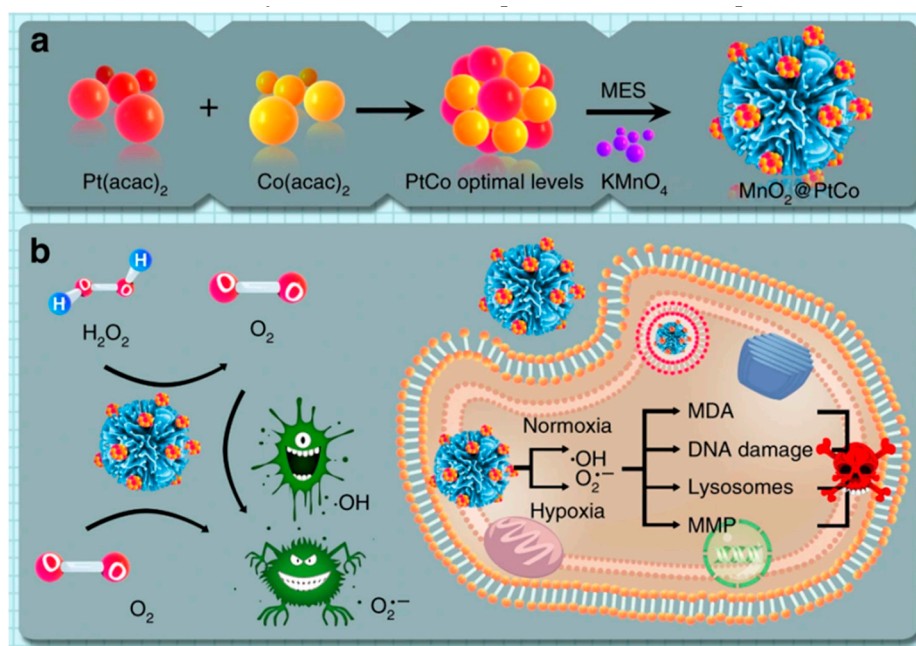


**Figure 8.** Schematic representation of (a) the synthesis of MnO<sub>2</sub>@PtCo nanoflowers and (b) the generation mechanism of reactive oxygen species (ROS) and cytotoxicity by MnO<sub>2</sub>@PtCo nanoflowers under different oxygen tensions. Reproduced from Reference [100] with permission from The Nature Publishing Group.

#### 5. Summary and Outlook

The emergence of nanozymes not only changes the traditional concept that nanomaterials are biological inert substances, but also provides a new perspective for the study of the biological effects of nanomaterials. Nanozymes enrich the research content of enzyme mimics, making it expand

from organic compounds to inorganic nanomaterials, expanding the application of nanomaterials. Although tremendous progress has been achieved in the field of nanozymes, this field still faces great challenges. Firstly, the catalytic mechanism of different kinds of nanozymes should be thoroughly investigated. Generally, the nanozymes exhibit multiple enzyme-mimicking catalytic properties due to the diversity of substrates. Therefore, the catalytic specificity and substrate selectivity of the nanozyme should be regulated and explored for designing different applications. With the development of nanotechnology, numerous and new discoveries of nanozymes should be explored, expanding the scope of enzyme categories. Future designs will be focused on reversibly turning ON/OFF the catalytic activity of nanozymes by changing the environmental condition. Nanozymes possess dual-functional characteristics as nanomaterials with catalytic properties. It is possible, by means of combining the dual functional characteristics of nanozymes, to create more nanozymes with unique functions and reveal their mechanisms of action that can be applied to human health, environmental protection, and bioenergy in the future.

**Funding:** This research was funded by the National Natural Science Foundation of China (21575031, 21964004), the Natural Science Foundation of Guangxi (2018GXNSFBA050053, 2018GXNSFBA281053, AD19110004), the Key Project of Guangxi Normal University (2017ZD003, 2017ZD005), the Open Project Program of Key Laboratory for Analytical Science of Food Safety and Biology, the Ministry of Education and the Program for BAGUI Scholar. And the APC was funded by the National Natural Science Foundation of China [21964004].

**Acknowledgments:** The authors are grateful to Dianping Tang and Liangqia Guo for substantive support.

**Conflicts of Interest:** The author(s) declare that they have no competing interest.

## References

1. Breslow, R. *Artificial enzymes*; Wiley-VCH Verlag GmbH & Co. KGaA: Weinheim, Germany, 2005; pp. 1–35.
2. Breslow, R.; Overman, L.E. "Artificial enzyme" combining a metal catalytic group and a hydrophobic binding cavity. *J. Am. Chem. Soc.* **1970**, *92*, 1075–1077. [[CrossRef](#)]
3. Xiong, X.; Huang, Y.; Lin, C.; Liu, X.Y.; Lin, Y. Recent advances in nanoparticulate biomimetic catalysts for combating bacteria and biofilms. *Nanoscale* **2019**, *11*, 22206–22215. [[CrossRef](#)]
4. Wu, J.; Wang, X.; Wang, Q.; Lou, Z.; Li, S.; Zhu, Y.; Qin, L.; Wei, H. Nanomaterials with enzyme-like characteristics (nanozymes): Next-generation artificial enzymes (II). *Chem. Soc. Rev.* **2019**, *48*, 1004–1076. [[CrossRef](#)]
5. Wei, H.; Wang, E. Nanomaterials with enzyme-like characteristics (nanozymes): Next-generation artificial enzymes. *Chem. Soc. Rev.* **2013**, *42*, 6060–6093. [[CrossRef](#)]
6. Wang, X.; Hu, Y.; Wei, H. Nanozymes in bionanotechnology: From sensing to therapeutics and beyond. *Inorg. Chem. Front.* **2016**, *3*, 41–60. [[CrossRef](#)]
7. Manea, F.; Houillon, F.B.; Pasquato, L.; Scrimin, P. Nanozymes: Gold-nanoparticle-based transphosphorylation catalysts. *Angew. Chem. Int. Ed.* **2004**, *43*, 6165–6169. [[CrossRef](#)]
8. Gao, L.; Zhuang, J.; Nie, L.; Zhang, J.; Zhang, Y.; Gu, N.; Wang, T.; Feng, J.; Yang, D.; Perrett, S. Intrinsic peroxidase-like activity of ferromagnetic nanoparticles. *Nat. Nanotechnol.* **2007**, *2*, 577. [[CrossRef](#)]
9. Chen, Y.; Cao, H.; Shi, W.; Liu, H.; Huang, Y. Fe–Co bimetallic alloy nanoparticles as a highly active peroxidase mimetic and its application in biosensing. *Chem. Commun.* **2013**, *49*, 5013–5015. [[CrossRef](#)]
10. Shi, W.; Wang, Q.; Long, Y.; Cheng, Z.; Chen, S.; Zheng, H.; Huang, Y. Carbon nanodots as peroxidase mimetics and their applications to glucose detection. *Chem. Commun.* **2011**, *47*, 6695–6697. [[CrossRef](#)]
11. Long, Y.J.; Li, Y.F.; Liu, Y.; Zheng, J.J.; Tang, J.; Huang, C.Z. Visual observation of the mercury-stimulated peroxidase mimetic activity of gold nanoparticles. *Chem. Commun.* **2011**, *47*, 11939–11941. [[CrossRef](#)]
12. Liu, S.; Tian, J.; Wang, L.; Luo, Y.; Sun, X. A general strategy for the production of photoluminescent carbon nitride dots from organic amines and their application as novel peroxidase-like catalysts for colorimetric detection of H<sub>2</sub>O<sub>2</sub> and glucose. *Rsc Adv.* **2012**, *2*, 411–413. [[CrossRef](#)]
13. Nirala, N.R.; Abraham, S.; Kumar, V.; Bansal, A.; Srivastava, A.; Saxena, P.S. Colorimetric detection of cholesterol based on highly efficient peroxidase mimetic activity of graphene quantum dots. *Sens. Actuators B Chem.* **2015**, *218*, 42–50. [[CrossRef](#)]

14. Wang, H.; Liu, C.; Liu, Z.; Ren, J.; Qu, X. Specific oxygenated groups enriched graphene quantum dots as highly efficient enzyme mimics. *Small* **2018**, *14*, 1703710. [[CrossRef](#)]
15. Chen, Q.; Liu, M.; Zhao, J.; Peng, X.; Chen, X.; Mi, N.; Yin, B.; Li, H.; Zhang, Y.; Yao, S. Water-dispersible silicon dots as a peroxidase mimetic for the highly-sensitive colorimetric detection of glucose. *Chem. Commun.* **2014**, *50*, 6771–6774. [[CrossRef](#)]
16. Lin, Y.; Ren, J.; Qu, X. Nano-gold as artificial enzymes: Hidden talents. *Adv. Mater.* **2014**, *26*, 4200–4217. [[CrossRef](#)]
17. Shen, X.; Liu, W.; Gao, X.; Lu, Z.; Wu, X.; Gao, X. Mechanisms of oxidase and superoxide dismutation-like activities of gold, silver, platinum, and palladium, and their alloys: A general way to the activation of molecular oxygen. *J. Am. Chem. Soc.* **2015**, *137*, 15882–15891. [[CrossRef](#)]
18. Yu, C.J.; Chen, T.H.; Jiang, J.Y.; Tseng, W.L. Lysozyme-directed synthesis of platinum nanoclusters as a mimic oxidase. *Nanoscale* **2014**, *6*, 9618–9624. [[CrossRef](#)]
19. Luo, W.; Zhu, C.; Su, S.; Li, D.; He, Y.; Huang, Q.; Fan, C. Self-catalyzed, self-limiting growth of glucose oxidase-mimicking gold nanoparticles. *ACS Nano* **2010**, *4*, 7451–7458. [[CrossRef](#)]
20. Natalio, F.; André, R.; Hartog, A.F.; Stoll, B.; Jochum, K.P.; Wever, R.; Tremel, W. Vanadium pentoxide nanoparticles mimic vanadium haloperoxidases and thwart biofilm formation. *Nat. Nanotechnol.* **2012**, *7*, 530–535. [[CrossRef](#)]
21. Tian, Z.; Li, J.; Zhang, Z.; Gao, W.; Zhou, X.; Qu, Y. Highly sensitive and robust peroxidase-like activity of porous nanorods of ceria and their application for breast cancer detection. *Biomaterials* **2015**, *59*, 116–124. [[CrossRef](#)] [[PubMed](#)]
22. Korschelt, K.; Schwidetzky, R.; Pfitzner, F.; Strugatchi, J.; Schilling, C.; von der Au, M.; Kirchhoff, K.; Panthöfer, M.; Lieberwirth, I.; Tahir, M. CeO<sub>2-x</sub> nanorods with intrinsic urease-like activity. *Nanoscale* **2018**, *10*, 13074–13082. [[CrossRef](#)] [[PubMed](#)]
23. Li, J.; Liu, W.; Wu, X.; Gao, X. Mechanism of pH-switchable peroxidase and catalase-like activities of gold, silver, platinum and palladium. *Biomaterials* **2015**, *48*, 37–44. [[CrossRef](#)] [[PubMed](#)]
24. Wang, H.; Li, P.; Yu, D.; Zhang, Y.; Wang, Z.; Liu, C.; Qiu, H.; Liu, Z.; Ren, J.; Qu, X. Unraveling the enzymatic activity of oxygenated carbon nanotubes and their application in the treatment of bacterial infections. *Nano Lett.* **2018**, *18*, 3344–3351. [[CrossRef](#)] [[PubMed](#)]
25. André, R.; Natálio, F.; Humanes, M.; Leppin, J.; Heinze, K.; Wever, R.; Schröder, H.C.; Müller, W.E.; Tremel, W. V<sub>2</sub>O<sub>5</sub> nanowires with an intrinsic peroxidase-like activity. *Adv. Funct. Mater.* **2011**, *21*, 501–509. [[CrossRef](#)]
26. Vernekar, A.A.; Sinha, D.; Srivastava, S.; Paramasivam, P.U.; D'Silva, P.; Muges, G. An antioxidant nanozyme that uncovers the cytoprotective potential of vanadia nanowires. *Nat. Commun.* **2014**, *5*, 5301. [[CrossRef](#)]
27. Song, Y.; Qu, K.; Zhao, C.; Ren, J.; Qu, X. Graphene oxide: Intrinsic peroxidase catalytic activity and its application to glucose detection. *Adv. Mater.* **2010**, *22*, 2206–2210. [[CrossRef](#)]
28. Lin, T.; Zhong, L.; Wang, J.; Guo, L.; Wu, H.; Guo, Q.; Fu, F.; Chen, G. Graphite-like carbon nitrides as peroxidase mimetics and their applications to glucose detection. *Biosens. Bioelectron.* **2014**, *59*, 89–93. [[CrossRef](#)]
29. Zeb, A.; Xie, X.; Yousaf, A.B.; Imran, M.; Wen, T.; Wang, Z.; Guo, H.L.; Jiang, Y.F.; Qazi, I.A.; Xu, A.W. Highly efficient fenton and enzyme-mimetic activities of mixed-phase VO<sub>x</sub> nanoflakes. *ACS Appl. Mater. Interfaces* **2016**, *8*, 30126–30132. [[CrossRef](#)]
30. Lin, T.; Zhong, L.; Guo, L.; Fu, F.; Chen, G. Seeing diabetes: Visual detection of glucose based on the intrinsic peroxidase-like activity of MoS<sub>2</sub> nanosheets. *Nanoscale* **2014**, *6*, 11856–11862. [[CrossRef](#)]
31. Lin, T.; Zhong, L.; Song, Z.; Guo, L.; Wu, H.; Guo, Q.; Chen, Y.; Fu, F.; Chen, G. Visual detection of blood glucose based on peroxidase-like activity of WS<sub>2</sub> nanosheets. *Biosens. Bioelectron.* **2014**, *62*, 302–307. [[CrossRef](#)] [[PubMed](#)]
32. Huang, X.-W.; Wei, J.-J.; Liu, T.; Zhang, X.L.; Bai, S.M.; Yang, H.H. Silk fibroin-assisted exfoliation and functionalization of transition metal dichalcogenide nanosheets for antibacterial wound dressings. *Nanoscale* **2017**, *9*, 17193–17198. [[CrossRef](#)] [[PubMed](#)]
33. Chen, T.; Wu, X.; Wang, J.; Yang, G. WSe<sub>2</sub> few layers with enzyme mimic activity for high-sensitive and high-selective visual detection of glucose. *Nanoscale* **2017**, *9*, 11806–11813. [[CrossRef](#)] [[PubMed](#)]
34. Wu, X.; Chen, T.; Wang, J.; Yang, G. Few-layered MoSe<sub>2</sub> nanosheets as an efficient peroxidase nanozyme for highly sensitive colorimetric detection of H<sub>2</sub>O<sub>2</sub> and xanthine. *J. Mater. Chem. B* **2018**, *6*, 105–111. [[CrossRef](#)]

35. Xiong, Y.; Chen, S.; Ye, F.; Su, L.; Zhang, C.; Shen, S.; Zhao, S. Synthesis of a mixed valence state Ce-MOF as an oxidase mimetic for the colorimetric detection of biothiols. *Chem. Commun.* **2015**, *51*, 4635–4638. [[CrossRef](#)] [[PubMed](#)]
36. Yang, H.; Yang, R.; Zhang, P.; Qin, Y.; Chen, T.; Ye, F. A bimetallic (Co/2Fe) metal-organic framework with oxidase and peroxidase mimicking activity for colorimetric detection of hydrogen peroxide. *Microchim. Acta* **2017**, *184*, 4629–4635. [[CrossRef](#)]
37. Lin, T.; Qin, Y.; Huang, Y.; Yang, R.; Hou, L.; Ye, F.; Zhao, S. A label-free fluorescence assay for hydrogen peroxide and glucose based on the bifunctional MIL-53 (Fe) nanozyme. *Chem. Commun.* **2018**, *54*, 1762–1765. [[CrossRef](#)]
38. Zhang, J.W.; Zhang, H.T.; Du, Z.Y.; Wang, X.; Yu, S.H.; Jiang, H.L. Water-stable metal-organic frameworks with intrinsic peroxidase-like catalytic activity as a colorimetric biosensing platform. *Chem. Commun.* **2014**, *50*, 1092–1094. [[CrossRef](#)]
39. Wang, Y.; Zhu, Y.; Binyam, A.; Liu, M.; Wu, Y.; Li, F. Discovering the enzyme mimetic activity of metal-organic framework (MOF) for label-free and colorimetric sensing of biomolecules. *Biosens. Bioelectron.* **2016**, *86*, 432–438. [[CrossRef](#)]
40. Tan, H.; Li, Q.; Zhou, Z.; Ma, C.; Song, Y.; Xu, F.; Wang, L. A sensitive fluorescent assay for thiamine based on metal-organic frameworks with intrinsic peroxidase-like activity. *Anal. Chim. Acta* **2015**, *856*, 90–95. [[CrossRef](#)]
41. Liu, Y.L.; Zhao, X.J.; Yang, X.X.; Li, Y.F. A nanosized metal-organic framework of Fe-MIL-88NH<sub>2</sub> as a novel peroxidase mimic used for colorimetric detection of glucose. *Analyst* **2013**, *138*, 4526–4531. [[CrossRef](#)] [[PubMed](#)]
42. Wang, X.; Cao, W.; Qin, L.; Lin, T.; Chen, W.; Lin, S.; Yao, J.; Zhao, X.; Zhou, M.; Hang, C. Boosting the peroxidase-like activity of nanostructured nickel by inducing its 3+ oxidation state in LaNiO<sub>3</sub> perovskite and its application for biomedical assays. *Theranostics* **2017**, *7*, 2277. [[CrossRef](#)] [[PubMed](#)]
43. Ai, L.; Li, L.; Zhang, C.; Fu, J.; Jiang, J. MIL-53 (Fe): A metal-organic framework with intrinsic peroxidase-like catalytic activity for colorimetric biosensing. *Chem. Eur. J.* **2013**, *19*, 15105–15108. [[CrossRef](#)] [[PubMed](#)]
44. Baldim, V.; Bedioui, F.; Mignet, N.; Margail, I.; Berret, J.F. The enzyme-like catalytic activity of cerium oxide nanoparticles and its dependency on Ce<sup>(3+)</sup> surface area concentration. *Nanoscale* **2018**, *10*, 6971–6980. [[CrossRef](#)] [[PubMed](#)]
45. Zhang, W.; Dong, J.; Wu, Y.; Cao, P.; Song, L.; Ma, M.; Gu, N.; Zhang, Y. Shape-dependent enzyme-like activity of Co<sub>3</sub>O<sub>4</sub> nanoparticles and their conjugation with his-tagged EGFR single-domain antibody. *Colloid. Surf. B* **2017**, *154*, 55–62. [[CrossRef](#)] [[PubMed](#)]
46. Li, P.; Klet, R.C.; Moon, S.-Y.; Wang, T.C.; Deria, P.; Peters, A.W.; Klahr, B.M.; Park, H.J.; Al-Juaid, S.S.; Hupp, J.T. Synthesis of nanocrystals of Zr-based metal-organic frameworks with csq-net: Significant enhancement in the degradation of a nerve agent simulant. *Chem. Commun.* **2015**, *51*, 10925–10928. [[CrossRef](#)]
47. Peng, F.F.; Zhang, Y.; Gu, N. Size-dependent peroxidase-like catalytic activity of Fe<sub>3</sub>O<sub>4</sub> nanoparticles. *Chin. Chem. Lett.* **2008**, *19*, 730–733. [[CrossRef](#)]
48. Asati, A.; Santra, S.; Kaittanis, C.; Nath, S.; Perez, J.M. Oxidase-like activity of polymer-coated cerium oxide nanoparticles. *Angew. Chem. Int. Ed.* **2009**, *48*, 2308–2312. [[CrossRef](#)]
49. Ge, C.; Fang, G.; Shen, X.; Chong, Y.; Wamer, W.G.; Gao, X.; Chai, Z.; Chen, C.; Yin, J.J. Facet energy versus enzyme-like activities: The unexpected protection of palladium nanocrystals against oxidative damage. *ACS Nano* **2016**, *10*, 10436–10445. [[CrossRef](#)]
50. Peterson, G.W.; Lu, A.X.; Epps, T.H., III. Tuning the morphology and activity of electrospun polystyrene/UiO-66-NH<sub>2</sub> metal-organic framework composites to enhance chemical warfare agent removal. *ACS Appl. Mater. Interfaces* **2017**, *9*, 32248–32254. [[CrossRef](#)]
51. Singh, N.; Geethika, M.; Eswarappa, S.M.; Muges, G. Manganese-based nanozymes: Multienzyme redox activity and effect on the nitric oxide produced by endothelial nitric oxide synthase. *Chem. Eur. J.* **2018**, *24*, 8393–8403. [[CrossRef](#)] [[PubMed](#)]
52. Fang, G.; Li, W.; Shen, X.; Perez-Aguilar, J.M.; Chong, Y.; Gao, X.; Chai, Z.; Chen, C.; Ge, C.; Zhou, R. Differential Pd-nanocrystal facets demonstrate distinct antibacterial activity against Gram-positive and Gram-negative bacteria. *Nat. Commun.* **2018**, *9*, 129. [[CrossRef](#)] [[PubMed](#)]
53. Tian, R.; Sun, J.; Qi, Y.; Zhang, B.; Guo, S.; Zhao, M. Influence of VO<sub>2</sub> nanoparticle morphology on the colorimetric assay of H<sub>2</sub>O<sub>2</sub> and glucose. *Nanomaterials* **2017**, *7*, 347. [[CrossRef](#)] [[PubMed](#)]

54. Singh, N.; Savanur, M.A.; Srivastava, S.; D'Silva, P.; Muges, G. A redox modulatory  $Mn_3O_4$  nanozyme with multi-enzyme activity provides efficient cytoprotection to human cells in a Parkinson's disease model. *Angew. Chem. Int. Ed.* **2017**, *56*, 14267–14271. [[CrossRef](#)]
55. Mu, J.; Zhang, L.; Zhao, M.; Wang, Y. Catalase mimic property of  $Co_3O_4$  nanomaterials with different morphology and its application as a calcium sensor. *ACS Appl. Mater. Interfaces* **2014**, *6*, 7090–7098. [[CrossRef](#)]
56. Liu, S.; Lu, F.; Xing, R.; Zhu, J.J. Structural effects of  $Fe_3O_4$  nanocrystals on peroxidase-like activity. *Chem. Eur. J.* **2011**, *17*, 620–625. [[CrossRef](#)]
57. Wan, Y.; Qi, P.; Zhang, D.; Wu, J.; Wang, Y. Manganese oxide nanowire-mediated enzyme-linked immunosorbent assay. *Biosens. Bioelectron.* **2012**, *33*, 69–74. [[CrossRef](#)]
58. Zhang, K.; Zuo, W.; Wang, Z.; Liu, J.; Li, T.; Wang, B.; Yang, Z. A simple route to  $CoFe_2O_4$  nanoparticles with shape and size control and their tunable peroxidase-like activity. *Rsc Adv.* **2015**, *5*, 10632–10640. [[CrossRef](#)]
59. Singh, S.; Dosani, T.; Karakoti, A.S.; Kumar, A.; Seal, S.; Self, W.T. A phosphate-dependent shift in redox state of cerium oxide nanoparticles and its effects on catalytic properties. *Biomaterials* **2011**, *32*, 6745–6753. [[CrossRef](#)]
60. Lee, Y.; Garcia, M.A.; Frey Huls, N.A.; Sun, S. Synthetic tuning of the catalytic properties of  $Au-Fe_3O_4$  nanoparticles. *Angew. Chem. Int. Ed.* **2010**, *49*, 1271–1274. [[CrossRef](#)]
61. Fernandez-Garcia, S.; Jiang, L.; Tinoco, M.; Hungria, A.B.; Han, J.; Blanco, G.; Calvino, J.J.; Chen, X. Enhanced hydroxyl radical scavenging activity by doping lanthanum in ceria nanocubes. *J. Phys. Chem. C* **2016**, *120*, 1891–1901. [[CrossRef](#)]
62. Long, L.; Liu, J.; Lu, K.; Zhang, T.; Xie, Y.; Ji, Y.; Wu, X. Highly sensitive and robust peroxidase-like activity of  $Au-Pt$  core/shell nanorod-antigen conjugates for measles virus diagnosis. *J. Nanobiotechnol.* **2018**, *16*, 46. [[CrossRef](#)] [[PubMed](#)]
63. Zhu, Z.; Guan, Z.; Jia, S.; Lei, Z.; Lin, S.; Zhang, H.; Ma, Y.; Tian, Z.Q.; Yang, C.J.  $Au@Pt$  nanoparticle encapsulated target-responsive hydrogel with volumetric bar-chart chip readout for quantitative point-of-care testing. *Angew. Chem. Int. Ed.* **2014**, *53*, 12503–12507.
64. Wu, J.; Qin, K.; Yuan, D.; Tan, J.; Qin, L.; Zhang, X.; Wei, H. Rational design of  $Au@Pt$  multibranching nanostructures as bifunctional nanozymes. *ACS Appl. Mater. Interfaces* **2018**, *10*, 12954–12959. [[CrossRef](#)] [[PubMed](#)]
65. Zhu, A.; Sun, K.; Petty, H.R. Titanium doping reduces superoxide dismutase activity, but not oxidase activity, of catalytic  $CeO_2$  nanoparticles. *Inorg. Chem. Commun.* **2012**, *15*, 235–237. [[CrossRef](#)]
66. Sun, H.; Jiao, X.; Han, Y.; Jiang, Z.; Chen, D. Synthesis of  $Fe_3O_4-Au$  Nanocomposites with Enhanced Peroxidase-Like Activity. *Eur. J. Inorg. Chem.* **2013**, *2013*, 109–114. [[CrossRef](#)]
67. Wang, C.; Qian, J.; Wang, K.; Yang, X.; Liu, Q.; Hao, N.; Wang, C.; Dong, X.; Huang, X. Colorimetric aptasensing of ochratoxin A using  $Au@Fe_3O_4$  nanoparticles as signal indicator and magnetic separator. *Biosens. Bioelectron.* **2016**, *77*, 1183–1191. [[CrossRef](#)]
68. Ge, C.; Wu, R.; Chong, Y.; Fang, G.; Jiang, X.; Pan, Y.; Chen, C.; Yin, J.J. Synthesis of  $Pt$  hollow nanodendrites with enhanced peroxidase-like activity against bacterial infections: Implication for wound healing. *Adv. Funct. Mater.* **2018**, *28*, 1801484. [[CrossRef](#)]
69. Zhang, X.-Q.; Gong, S.-W.; Zhang, Y.; Yang, T.; Wang, C.-Y.; Gu, N. Prussian blue modified iron oxide magnetic nanoparticles and their high peroxidase-like activity. *J. Mater. Chem.* **2010**, *20*, 5110–5116. [[CrossRef](#)]
70. Sobańska, K.; Pietrzyk, P.; Sojka, Z. Generation of reactive oxygen species via electroprotic interaction of  $H_2O_2$  with  $ZrO_2$  gel: Ionic sponge effect and pH-switchable peroxidase-and catalase-like activity. *ACS Catal.* **2017**, *7*, 2935–2947. [[CrossRef](#)]
71. Zhang, W.; Hu, S.; Yin, J.J.; He, W.; Lu, W.; Ma, M.; Gu, N.; Zhang, Y. Prussian blue nanoparticles as multienzyme mimetics and reactive oxygen species scavengers. *J. Am. Chem. Soc.* **2016**, *138*, 5860–5865. [[CrossRef](#)] [[PubMed](#)]
72. Wang, T.; Su, P.; Li, H.; Yang, Y.; Yang, Y. Triple-enzyme mimetic activity of  $Co_3O_4$  nanotubes and their applications in colorimetric sensing of glutathione. *New J. Chem.* **2016**, *40*, 10056–10063. [[CrossRef](#)]
73. Fan, Y.; Shi, W.; Zhang, X.; Huang, Y. Mesoporous material-based manipulation of the enzyme-like activity of  $CoFe_2O_4$  nanoparticles. *J. Mater. Chem. A* **2014**, *2*, 2482–2486. [[CrossRef](#)]
74. Huang, Y.; Ran, X.; Lin, Y.; Ren, J.; Qu, X. Self-assembly of an organic-inorganic hybrid nanoflower as an efficient biomimetic catalyst for self-activated tandem reactions. *Chem. Commun.* **2015**, *51*, 4386–4389. [[CrossRef](#)]

75. Xu, C.; Bing, W.; Wang, F.; Ren, J.; Qu, X. Versatile dual photoresponsive system for precise control of chemical reactions. *ACS Nano* **2017**, *11*, 7770–7780. [[CrossRef](#)]
76. Sun, Z.; Zhang, N.; Si, Y.; Li, S.; Wen, J.; Zhu, X.; Wang, H. High-throughput colorimetric assays for mercury (II) in blood and wastewater based on the mercury-stimulated catalytic activity of small silver nanoparticles in a temperature-switchable gelatin matrix. *Chem. Commun.* **2014**, *50*, 9196–9199. [[CrossRef](#)]
77. Wu, G.W.; He, S.B.; Peng, H.P.; Deng, H.H.; Liu, A.L.; Lin, X.H.; Xia, X.H.; Chen, W. Citrate-capped platinum nanoparticle as a smart probe for ultrasensitive mercury sensing. *Anal. Chem.* **2014**, *86*, 10955–10960. [[CrossRef](#)]
78. Sun, Y.; Wang, J.; Li, W.; Zhang, J.; Zhang, Y.; Fu, Y. DNA-stabilized bimetallic nanozyme and its application on colorimetric assay of biothiols. *Biosens. Bioelectron.* **2015**, *74*, 1038–1046. [[CrossRef](#)]
79. Carmona, U.; Zhang, L.; Li, L.; Münchgesang, W.; Pippel, E.; Knez, M. Tuning, inhibiting and restoring the enzyme mimetic activities of Pt–apoferritin. *Chem. Commun.* **2014**, *50*, 701–703. [[CrossRef](#)]
80. Liu, J.; Hu, X.; Hou, S.; Wen, T.; Liu, W.; Zhu, X.; Wu, X. Screening of inhibitors for oxidase mimics of Au@ Pt nanorods by catalytic oxidation of OPD. *Chem. Commun.* **2011**, *47*, 10981–10983. [[CrossRef](#)]
81. Bing, W.; Sun, H.; Yan, Z.; Ren, J.; Qu, X. Programmed bacteria death induced by carbon dots with different surface charge. *Small* **2016**, *12*, 4713–4718. [[CrossRef](#)]
82. Cormode, D.P.; Gao, L.; Koo, H. Emerging biomedical applications of enzyme-like catalytic nanomaterials. *Trends Biotechnol.* **2018**, *36*, 15–29. [[CrossRef](#)]
83. Chen, Z.; Wang, Z.; Ren, J.; Qu, X. Enzyme mimicry for combating bacteria and biofilms. *Acc. Chem. Res.* **2018**, *51*, 789–799. [[CrossRef](#)]
84. Karim, M.N.; Singh, M.; Weerathunge, P.; Bian, P.; Zheng, R.; Dekiwadia, C.; Ahmed, T.; Walia, S.; Della Gaspera, E.; Singh, S. Visible-light-triggered reactive-oxygen-species-mediated antibacterial activity of peroxidase-mimic CuO nanorods. *ACS Appl. Nano Mater.* **2018**, *1*, 1694–1704. [[CrossRef](#)]
85. Xu, B.; Wang, H.; Wang, W.; Gao, L.; Li, S.; Pan, X.; Wang, H.; Yang, H.; Meng, X.; Wu, Q. A single-atom nanozyme for wound disinfection applications. *Angew. Chem. Int. Ed.* **2019**, *58*, 4911–4916. [[CrossRef](#)]
86. Hu, L.; Zhang, C.; Zeng, G.; Chen, G.; Wan, J.; Guo, Z.; Wu, H.; Yu, Z.; Zhou, Y.; Liu, J. Metal-based quantum dots: Synthesis, surface modification, transport and fate in aquatic environments and toxicity to microorganisms. *Rsc Adv.* **2016**, *6*, 78595–78610. [[CrossRef](#)]
87. Zhou, C.; Lai, C.; Xu, P.; Zeng, G.; Huang, D.; Zhang, C.; Cheng, M.; Hu, L.; Wan, J.; Liu, Y. In situ grown AgI/Bi<sub>2</sub>O<sub>3</sub>/Cl<sub>2</sub> heterojunction photocatalysts for visible light degradation of sulfamethazine: Efficiency, pathway, and mechanism. *ACS Sustain. Chem. Eng.* **2018**, *6*, 4174–4184. [[CrossRef](#)]
88. Wan, J.; Zeng, G.; Huang, D.; Hu, L.; Xu, P.; Huang, C.; Deng, R.; Xue, W.; Lai, C.; Zhou, C. Rhamnolipid stabilized nano-chlorapatite: Synthesis and enhancement effect on Pb- and Cd-immobilization in polluted sediment. *J. Hazard. Mater.* **2018**, *343*, 332–339. [[CrossRef](#)]
89. Jiang, J.; He, C.; Wang, S.; Jiang, H.; Li, J.; Li, L. Recyclable ferromagnetic chitosan nanozyme for decomposing phenol. *Carbohydr. Polym.* **2018**, *198*, 348–353. [[CrossRef](#)]
90. Wang, J.; Huang, R.; Qi, W.; Su, R.; Binks, B.P.; He, Z. Construction of a bioinspired laccase-mimicking nanozyme for the degradation and detection of phenolic pollutants. *Appl. Catal. B* **2019**, *254*, 452–462. [[CrossRef](#)]
91. Liu, B.; Liu, J. Surface modification of nanozymes. *Nano Res.* **2017**, *10*, 1125–1148. [[CrossRef](#)]
92. Zhang, S.; Lin, F.; Yuan, Q.; Liu, J.; Li, Y.; Liang, H. Robust magnetic laccase-mimicking nanozyme for oxidizing o-phenylenediamine and removing phenolic pollutants. *J. Environ. Sci. (China)* **2020**, *88*, 103–111. [[CrossRef](#)]
93. Miller, E.B.; Zahran, E.M.; Knecht, M.R.; Bachas, L.G. Metal oxide semiconductor nanomaterial for reductive debromination: Visible light degradation of polybrominated diphenyl ethers by Cu<sub>2</sub>O@ Pd nanostructures. *Appl. Catal. B* **2017**, *213*, 147–154. [[CrossRef](#)]
94. Fan, G.; Zhan, J.; Luo, J.; Zhang, J.; Chen, Z.; You, Y. Photocatalytic degradation of naproxen by a H<sub>2</sub>O<sub>2</sub>-modified titanate nanomaterial under visible light irradiation. *Catal. Sci. Technol.* **2019**, *9*, 4614–4628. [[CrossRef](#)]
95. Qiu, H.; Pu, F.; Ran, X.; Liu, C.; Ren, J.; Qu, X. Nanozyme as artificial receptor with multiple readouts for pattern recognition. *Anal. Chem.* **2018**, *90*, 11775–11779. [[CrossRef](#)]

96. Hou, L.; Qin, Y.; Li, J.; Qin, S.; Huang, Y.; Lin, T.; Guo, L.; Ye, F.; Zhao, S. A ratiometric multicolor fluorescence biosensor for visual detection of alkaline phosphatase activity via a smartphone. *Biosens. Bioelectron.* **2019**, *143*, 111605. [[CrossRef](#)]
97. Wang, X.; Qin, L.; Lin, M.; Xing, H.; Wei, H. Fluorescent graphitic carbon nitride-based nanozymes with peroxidase-like activities for ratiometric biosensing. *Anal. Chem.* **2019**, *91*, 10648–10656. [[CrossRef](#)]
98. Jiang, D.; Ni, D.; Rosenkrans, Z.T.; Huang, P.; Yan, X.; Cai, W. Nanozyme: New horizons for responsive biomedical applications. *Chem. Soc. Rev.* **2019**, *48*, 3683–3704. [[CrossRef](#)]
99. Li, S.; Shang, L.; Xu, B.; Wang, S.; Gu, K.; Wu, Q.; Sun, Y.; Zhang, Q.; Yang, H.; Zhang, F. A Nanozyme with Photo-Enhanced Dual Enzyme-Like Activities for Deep Pancreatic Cancer Therapy. *Angew. Chem. Int. Ed.* **2019**, *58*, 12624–12631. [[CrossRef](#)]
100. Wang, Z.; Zhang, Y.; Ju, E.; Liu, Z.; Cao, F.; Chen, Z.; Ren, J.; Qu, X. Biomimetic nanoflowers by self-assembly of nanozymes to induce intracellular oxidative damage against hypoxic tumors. *Nat. Commun.* **2018**, *9*, 3334. [[CrossRef](#)]



© 2019 by the authors. Licensee MDPI, Basel, Switzerland. This article is an open access article distributed under the terms and conditions of the Creative Commons Attribution (CC BY) license (<http://creativecommons.org/licenses/by/4.0/>).